Influence of light illumination on the potential-induced degradation of n-type interdigitated back-contact crystalline Si photovoltaic modules

Yuansong Xu[1], Atsushi Masuda[2,3], and Keisuke Ohdaira[1]

[1]*Japan Advanced Insistute of Science and Technology, 1-1 Asahidai, Nomi, Ishikawa 923-1292, Japan*

[2]*National Institute of Advanced Industrial Science and Technology, 1-1-1 Umezono, Tsukuba, Ibaraki 305-8568, Japan*

[3]*Niigata University, 8050 Ikarashi 2-no-cho, Nishi-ku, Niigata 950-2181, Japan*

E-mail: ohdaira@jaist.ac.jp

We investigate the potential-induced degradation (PID) of n-type interdigitated back-contact (IBC) crystalline Si (c-Si) photovoltaic (PV) modules under a negative bias stress and the influence of light illumination on the PID. IBC PV modules show PID characterized by reductions in short-circuit current density (J_{sc}) and open-circuit voltage (V_{oc}) under negative bias stress, while no fill factor (FF) reduction is observed. The degradation may originate from sodium (Na) introduction into c-Si and resulting enhancement of carrier recombination on the surface of the IBC cells. 1-sun light illumination during the negative-bias PID test results in less severe reductions in J_{sc} and V_{oc}. A reduction in an electric field in the surface Si nitride (SiN_x) film due to carrier generation in the SiN_x and resulting increase in its conductivity is one of the possible explanations for the mitigation of the Na-related PID.

I. Introduction

Photovoltaic (PV) market has been rapidly growing these days, and crystalline silicon (c-Si) solar cells and modules have dominated the market share due to their matured fabrication technology and reducing electricity cost. n-type c-Si solar cells generally have higher efficiency than conventional p-type c-Si ones, and their widespread use is thus expected in the near future.[1,2] In particular, interdigitated back-contact (IBC) solar cells are known as high-efficiency solar cells because all the electrodes are formed on the rear surface of the cells and the light incident area can thus be enlarged, resulting in a larger photocurrent compared to conventional solar cells with electrodes on the illumination side.[3,4]

It is important to clarify the behavior and mechanism of the long-term reliability of PV modules with IBC cells. Potential-induced degradation (PID) is a performance degradation of PV modules triggered by a voltage between a grounded Al frame and cells,[5–39] and is one of the most important reliability issues because of its severity. The mechanism of the PID of c-Si PV modules with conventional p-type cells has been considerably clarified,[5–21] which show a reduction in fill factor (FF) under a negative bias stress, originating from the formation of shunting paths due to sodium (Na) introduction.[9–11] On the other hand, there have been relatively fewer previous studies on the PID of n-type c-Si PV modules.[23–39] Regarding the PID of the IBC PV modules,[23–26] reductions in open-circuit voltage (V_{oc}) and short-circuit current density (J_{sc}) occur when a positive bias is applied to the cells with respect to the grounded Al frame. This can be explained by the accumulation of negative charges in the front Si nitride (SiN_x) and resulting acceleration of carrier recombination on the surface. On the contrary, the PID of IBC PV modules under negative bias has not been fully investigated yet. Furthermore, since PID occurs only under sunlight illumination in the field, it is also important to clarify the influence of light illumination on the PID of IBC modules.

In this study, we investigate the PID of IBC PV modules under negative bias and the influence of light illumination on their PID. To clarify the PID of IBC PV modules under negative bias in more detail, in addition to our prior work,[39] we performed current density–voltage (J–V) measurement and its analysis to evaluate saturation current density, external quantum efficiency (EQE) measurement, and electroluminescence (EL) imaging.

2. Experimental Procedures

We laminated 12.5×12.5 cm^2-sized commercial homojunction IBC cells with an n^+ layer on the surface to fabricate one-cell modules with a structure of glass/ethylene vinyl acetate copolymer (EVA)/cell/EVA/backsheet. The size of the cover glass was 18×18 cm^2, and the EVA has a relatively low resistivity of 1.5×10^{15} Ω·cm. Al tapes were attached around the four sides of the modules to mimic the Al frame of a PV module. A PID test was conducted by applying −2000 V to the cells with respect to the grounded Al tape at a temperature of 85 °C. No intentional humidity stress was applied during the PID test. A thermocouple was attached to the back side of the modules during the test in order to check the temperature of the modules. The PID test in the dark was performed by connecting several IBC modules in parallel. We also performed the PID test under 1-sun light illumination to investigate the effects of light illumination. The PID test under light illumination was performed separately for each module.

For the evaluation of the performance degradation of the IBC PV modules by PID, *J*–*V* characteristics and EQE spectra were measured before and after the PID tests. The *J*–*V* characteristics were measured in the dark and 1-sun illumination, and the dark *J*–*V* curves were analyzed using the 2-diode model to obtain saturation current densities originating from diffusion and recombination currents, J_{01} and J_{02}, respectively. The EQE spectra were measured without bias light under a photon flux of the monochromatic light of 1.0×10^{14} /cm^2·s at several points of the IBC PV modules to evaluate the areal distribution of the degradation. The position dependence of the degradation was also characterized by capturing EL images of the IBC PV modules.

3. Results

Figure 1 shows the photo *J*–*V* curves of the IBC PV modules before and after the PID test for 10 days in the dark and under 1-sun light illumination. One can see reductions in the output power of the IBC PV modules by the PID stress. This result clearly demonstrates that IBC PV modules can degrade under negative-bias PID stress. No significant decrease in FF is observed in the *J*–*V* characteristics of the IBC PV modules after the PID tests. This is quite reasonable because the p–n junction exists on the rear side of the cell, far from the front-side surface exposed to the PID stress. On the contrary,

J_{sc} and V_{oc} significantly decrease in the IBC PV modules receiving the negative-bias PID stress. In addition, a large difference in the J–V curves of the IBC PV modules is seen depending on the presence or absence of 1-sun light illumination during the PID test; the module receiving the PID stress with 1-sun light illumination clearly shows smaller decreases in the J_{sc} and V_{oc} compared to the module undergoing the PID test without light illumination. This fact indicates that the PID of IBC PV modules under negative bias is mitigated by light illumination.

Figure 2 shows the J_{sc}, V_{oc}, FF, and maximum power (P_{max}), normalized by their initial values, of the IBC PV modules as a function of PID-stress duration. The results both for the PID test in the dark and under 1-sun light illumination are shown. The modules do not show any degradation within the first 30 minutes. J_{sc} and V_{oc} then start to reduce simultaneously, and their reductions are saturated at ~72 hours. The coincidence in the decreases in J_{sc} and V_{oc} may indicate that these degradations result from a common cause. FF does not deteriorate at all, as also mentioned above. The modules receiving 1-sun light illumination during the PID test clearly show a smaller P_{max} reduction than the modules undergoing PID test in the dark at all the PID test durations.

Figure 3 shows J_{01} and J_{02} obtained by the 2-diode fitting of the dark J–V curves of the IBC PV modules plotted as a function of PID-stress duration. J_{01} of the IBC PV modules start to increase after the PID test for ~30 min, which corresponds to the onset of V_{oc} reduction. 1-sun light illumination during the PID stress leads to the mitigation of J_{01} increase, similar to the change in V_{oc}. These indicate that the decrease in V_{oc} is strongly related to the increase in J_{01}. On the contrary, no significant change in J_{02} is seen. An increase in J_{02} generally indicates the increase in recombination current and coincides a decrease in FF due to increased ideality factor. The unchanged J_{02} is thus consistent with the fact that FF does not change by the PID stress. This may be peculiarity of the PID of IBC modules compared to the modules with cells with a p–n junction on their front side.

Figure 4 shows the EQE spectra of the IBC modules before and after the PID test in the dark and under 1-sun light illumination measured at the edge of the cells. The mitigation of PID by 1-sun light illumination is also confirmed by comparing the EQE spectra of the modules after 10-days PID test. Decreases in EQE in a whole wavelength region are confirmed. Such a decrease in the EQE in a wide wavelength region is sometimes explained by the increased optical loss on the cell surface.[33,34] This seems to be unlikely in this case because J_{sc} decreases with a decrease in V_{oc} and carrier recombination must lead to J_{sc} and EQE reductions. Figure 5 shows the EQE spectra of the IBC PV modules measured at the cell edge and at the center of the cell before and after the PID test in the dark. More serious EQE reduction is seen in the spectra measured at the cell edge. This means that PID does not occur uniformly and but occurs more seriously near the Al tapes. Stronger electric field near the Al tape may be the reason for the nonuniform EQE loss.

Figure 6 shows the EL images of the IBC PV module before and after the PID test in the dark. The EL intensity of the IBC module decreases with an increase in the PID-stress duration, and almost disappears by the PID test for 2 hours. We thus increased an injection current from 0.5 to 1 A and continued the PID test. Further increase in the PID-stress duration results in more significant decrease in the EL intensity. The decrease in the EL intensity is another clear indication of the emergence of PID in the IBC PV modules under negative bias stress. The EL images seem to be darker at the edges than at the center of the cell. This is consistent with the results of the EQE measurements, and is probably due to more degradation by stronger electric field at the cell edges during the PID stress.

4. Discussion

In general, the main causes for the PID of PV modules are (1) optical loss by the change of transparency of surface material, (2) charge accumulation in the front SiN_x, and (3) Na introduction into c-Si. Among them, as mentioned above, the possibility of optical loss can be safely excluded. The optical loss on the cell surface just reduces photo flux into c-Si, and thus, in general, results in a reduction in J_{sc} alone and almost no change in V_{oc}.[33,34] However, simultaneous reductions in J_{sc} and V_{oc} are seen in the PID of IBC PV modules, which coincide with an increase in J_{01}, as shown in Fig. 3. This suggests that an enhancement in carrier recombination is the main cause of the PID. Note that a reduction in J_{sc} to be less than half of its initial value, shown in Fig. 2, is possible in IBC cells if a surface recombination velocity on the front-side surface deteriorates to be ~1000 cm/s.[40]

We next discuss the possibility of PID induced by the charge accumulation. As shown in Figs. 1 and 2, the PID of IBC PV modules under negative bias is characterized by the reductions in J_{sc} and V_{oc}. These tendencies are actually observed in the other types of PV modules degraded by the accumulation of fixed charges,[27–32] the origin of which may be charged K centers, Si dangling bonds backbonded to three nitrogen atoms.[28,29] However, the PID of IBC modules by negative bias cannot be explained by the charge accumulation in SiN_x, according to the following two reasons. The IBC cells used in this study consist of an n-type c-Si absorber, in which holes are minority carriers. Accumulated in the SiN_x by applying a negative bias to a cell are positive charges, which rather reduces the concentration of the minority carrier (hole) density near the c-Si surface. Furthermore, PID induced by charge accumulation in SiN_x generally occurs more rapidly than the results obtained in this study. For example, J_{sc} and V_{oc} of n-type front-emitter PV modules start to drop within 1 min and then saturates within a few minutes at a bias voltage of −1000 V at 85 °C.[28,29] These time constants are completely different from the results in this study: ~30 min for the onset of the reductions in J_{sc} and V_{oc}. We can thus conclude that the PID of IBC cells is not induced by the charge accumulation in SiN_x.

Most feasible mechanism of the PID of IBC PV modules under negative bias is the introduction of Na into c-Si. It is well known that, in the PV modules with conventional p-type wafer-based cells, Na ions pass through the front SiN_x by the assistance of electric field and enter c-Si with the formation of Na-decorated stacking faults.[9–11] The Na-decorated stacking faults penetrate a surface n^+ emitter and act as shunting paths, resulting in a reduction in FF. Since the surface structure of IBC cells, containing SiN_x and an n^+ layer, is almost the same as that of the p-type conventional cells, Na introduction based on the similar mechanism can also occur on the surface of IBC cells. Since the p–n junction is on the rear side in the IBC cells, the Na-decorated stacking faults on the surface do not act as shunting paths but as recombination centers. They cause more carrier recombination on the front-side surface, leading to reductions in J_{sc} and V_{oc}. This explanation is consistent with the increase in J_{01}.

It may be seemingly curious that the EQE of IBC PV modules decreases not only in a short wavelength region but in an entire wavelength region, even due to the enhancement of the front-side surface recombination by Na introduction only near the surface. This can be explained by the sufficiently long minority carrier diffusion length in the IBC cells. Minority carriers, holes in n-type c-Si base, must have a diffusion length much larger than a wafer thickness. Otherwise, the minority carriers will recombine before reaching interdigitated p-type emitter regions with a pitch of several hundreds of μm. The long carrier diffusion length exceeding the wafer thickness allows the minority carriers generated even in the vicinity of the rear side of the cells to reach the front-side surface. Hence, all the excess minority carriers, wherever they are generated, can recombine on the front-side surface and EQE can be reduced in an entire wavelength region.

We finally discuss the mechanism of the mitigation of PID by light illumination. The mitigation of PID by light illumination has been reported for conventional p-type c-Si PV modules.[19–21] This is usually explained as a result of carrier excitation in SiN_x. Since the typical bandgap of SiN_x is ~3 eV,[21] ultraviolet light in 1-sun light can excite carriers in SiN_x and its conductivity increases. As a result, an electric field applied to SiN_x is weakened, leading to the less efficient drift of Na through SiN_x. This can also be one of the possible reasons for the mitigation of the PID of IBC modules under 1-sun light illumination, because of the similarity of the surface structures in conventional p-type cells and IBC cells. These findings about the PID of IBC PV modules under negative bias are useful to evaluate their long-term reliability in the field, where the modules receive PID stress with light illumination.

5. Conclusion

We investigated the PID of the IBC modules under negative bias and the effect of light illumination on their PID. As a result of a PID test for ~10 days, J_{sc} and V_{oc} decrease simultaneously, whereas FF is unchanged. By fitting the dark J–V curves, J_{01} is found to be increased with reductions in J_{sc} and V_{oc}. The most possible mechanism for the reductions in J_{sc} and V_{oc} is Na introduction into the cell surface and enhanced surface recombination of minority carriers. The EQE spectra of IBC PV modules change in an entire wavelength region. This is probably because of the large diffusion length of minority carriers exceeding a wafer thickness and resulting front-side surface recombination of carriers generated even near the rear side of the cells. We also confirmed that the PID of IBC PV modules under negative bias is mitigated by 1-sun light illumination. Weakened electric field in SiN_x by carrier excitation is a possible mechanism for the mitigation of PID, similar to the case of conventional p-type c-Si PV modules.

Acknowledgment

We would like to thank Ms. Yukiko Hara of National Institute of Advanced Industrial Science and Technology for her help for the experiments. This work was supported by the New Energy and Industrial Technology Development Organization (NEDO).

Reference

1) IEA-PVPS, “Trends in Photovoltaic Applications”, 2019.
2) A. ur Rehman and S. H. Lee, Sci. World J. **2013**, 470347 (2013).
3) D. D. Smith, G. Reich, M. Baldrias, M. Reich, N. Boitnott, and G. Bunea, Proc. 43rd IEEE Photovoltaic Specialists Conf., 2016, p. 3351.
4) K. Yoshikawa, H. Kawasaki, W. Yoshida, T. Irie, K. Konishi, K. Nakano, T. Uto, D. Adachi, M. Kanematsu, H. Uzu, and K. Yamamoto, Nat. Energy **2**, 17032 (2017).
5) W. Luo, Y. S. Khoo, P. Hacke, V. Naumann, D. Lausch, S. P. Harvey, J. P. Singh, J. Chai, Y. Wang, A. G. Aberle, and S. Ramakrishna, Energy Environ. Sci. **10**, 43 (2017).
6) S. Pingel, O. Frank, M. Winkler, S. Daryan, T. Geipel, H, Hoehne, and J. Berghold, Proc. 35th IEEE Photovoltaic Specialists Conf., 2010, p. 2817.
7) J. Berghold, O. Frank, H. Hoehne, S. Pingel, B. Richardson, and M. Winkler, Proc. 25th European Photovoltaic Solar Energy Conf. Exhib./5th World Conf. Photovoltaic Energy Conversion, 2010, p. 3753.
8) P. Hacke, M. Kempe, K. Terwilliger, S. Glick, N. Call, S. Johnston, S. Kurtz, I. Bennett, and M. Kloos, Proc. 25th European Photovoltaic Solar Energy Conf. Exhib./5th World Conf. Photovoltaic Energy Conversion, 2010, p. 3760.
9) V. Naumann, D. Lausch, A. Hähnel, J. Bauer, O. Breitenstein, A. Graff, M. Werner, S. Swatek, S. Großer, J. Bagdahn, and C. Hagendorf, Sol. Energy Mater. Sol. Cells **120**, 383 (2014).
10) V. Naumann, D. Lausch, and C. Hagendorf, Energy Procedia **77**, 397 (2015).
11) V. Naumann, C. Brzuska, M. Werner, S. Großer, and C. Hagendorf, Energy Procedia **92**, 569 (2016).
12) V. Naumann, C. Hagendorf, S. Grosser, M. Werner, and J. Bagdahn, Energy Procedia **27**, 1 (2012).
13) C. Taubitz, M. Schütze, and M. B. Koentopp, Proc. 27th European Photovoltaic Solar Energy Conf. Exhib., 2012, p. 3172.
14) H. Nagel, A. Metz, and K. Wangemann, Proc. 26th European Photovoltaic Solar Energy Conf. Exhib., 2011, p. 3107.

15) D. Lausch, V. Naumann, O. Breitenstein, J. Bauer, A. Graff, J. Bagdahn, and C. Hagendorf, IEEE J. Photovolt. **4**, 834 (2014).
16) S. Hoffmann and M. Koehl, Prog. Photovolt: Res. Appl. **22**, 173 (2014).
17) Z. Xiong, T. M. Walsh, and A. G. Aberle, Energy Procedia **8**, 384 (2011).
18) J. Bauer, V. Naumann, S. Großer, C. Hagendorf, M. Schütze, and O. Breitenstein, Phys. Status Solidi: Rapid Res. Lett. **6**, 331 (2012).
19) A. Masuda and Y. Hara, Jpn. J. Appl. Phys. **57**, 08RG13 (2018).
20) P. Hacke, K. Terwilliger, S. Glick, G. Tamizhmani, S. Tatapudi, C. Stark, S. Koch, T. Weber, J. Berghold, S. Hoffmann, M. Koehl, S. Dietrich, M. Ebert, and G. Mathiak, IEEE. J. Photovolt. **5**, 94 (2015).
21) D. C. Nguyen, Y. Ishikawa, S. Jonai, K. Nakamura, A. Masuda, and Y. Uraoka, Sol. Energy **199**, 55 (2020).
22) K. Hara, H. Ichinose, T. N. Murakami, and A. Masuda, RSC Adv. **4**, 44291 (2014).
23) R. Swanson, M. Cudzinovic, D. DeCeuster, V. Desai, J. Jürgens, N. Kaminar, W. Mulligan, L. Rodrigues-Barbosa, D. Rose, D. Smith, A. Terao, and K. Wilson, Ext. Abst. 15th Int. Photovoltaic Science Engineering Conf., 2005, p. 410.
24) V. Naumann, T. Geppert, S. Großer, D. Wichmann, H-J. Krokoszinski, M. Werner, and C. Hagendorf, Energy Procedia **55**, 498 (2014).
25) A. Halm, A. Schneider, V. D. Mihailetchi, L. J. Koduvelikulathu, L. M. Popescu, G. Galbiati, H. Chu, and R. Kopecek, Energy Procedia **77**, 356 (2015).
26) T. Ishii, S. Choi, R. Sato, Y. Chiba, and A. Masuda, Prog. Photovolt: Res. Appl. https://doi.org/10.1002/pip.3329.
27) K. Hara, S. Jonai, and A. Masuda, Sol. Energy Mater. Sol. Cells **140**, 361 (2015).
28) S. Yamaguchi, A. Masuda, and K. Ohdaira, Appl. Phys. Express **9**, 112301 (2016).
29) S. Yamaguchi, K. Nakamura, A. Masuda, and K. Ohdaira, Jpn. J. Appl. Phys. **57**, 122301 (2018).
30) S. Bae, W. Oh, K. D. Lee, S. Kim, H. Kim, N. Park, S.-I. Chan, S. Park, Y. Kang, H-S. Lee, and D. Kim, Energy Sci. Eng. **5**, 30 (2017).
31) M. Barbato, A. Barbato, M. Meneghini, G. Tavernaro, M. Rossetto, and G. Meneghesso, Sol. Energy Mater. Sol. Cells **168**, 51 (2017).
32) K. Hara, K. Ogawa, Y. Okabayashi, H. Matsuzaki, and A. Masuda, Sol. Energy Mater. Sol. Cells **166**, 132 (2017).

33) S. Yamaguchi, C. Yamamoto, K. Ohdaira, and A. Masuda, Sol. Energy Mater. Sol. Cells **161**, 439 (2017).

34) S. Yamaguchi, C. Yamamoto, K. Ohdaira, and A. Masuda, Prog. Photovolt: Res. Appl. **26**, 697 (2018).

35) Y. Komatsu, S. Yamaguchi, A. Masuda, and K. Ohdaira, Microelectron. Reliab. **84**, 127 (2018).

36) K. Ohdaira, Y. Komatsu, T. Suzuki, S. Yamaguchi, and A. Masuda, Appl. Phys. Express **12**, 064004 (2019).

37) T. Suzuki, S. Yamaguchi, K. Nakamura, A. Masuda, and K. Ohdaira, Jpn. J. Appl. Phys. **59**, SCCD02 (2020).

38) T. Suzuki, A. Masuda, and K. Ohdaira, Jpn. J. Appl. Phys. **59**, 104002 (2020).

39) Y. Xu, A. Masuda, and K. Ohdaira, Ext. Abst. 2020 Int. Conf. Solid State Devices and Materials (SSDM2020), 2020, p.401.

40) D. Diouf, J. P. Kleider, T. Desrues, and P.-J. Ribeyron, Mater. Sci. Eng. B **159–160**, 291 (2009).

Figure Captions

Fig. 1 Photo *J–V* curves of IBC PV modules before and after the PID test in the dark and under 1-sun light illumination.

Fig. 2 J_{sc}, V_{oc}, FF, and P_{max}, normalized by their initial values, of the IBC PV modules as a function of the duration of the PID test performed in the dark and under 1-sun light illumination. The open and closed dots indicate the data points from individual modules.

Fig. 3 J_{01} and J_{02} obtained by the 2-diode fitting of the dark *J–V* curves of the IBC PV modules as a function of PID-stress duration.

Fig. 4 EQE spectra of the IBC PV modules before and after the PID test in the dark and under 1-sun light illumination for 10 days measured at the cell edge.

Fig. 5 EQE spectra of the IBC PV modules (a) at the center and (b) at the edge of the cell before and after the PID test for 10 days in the dark.

Fig. 6 EL images of IBC PV module before and after the PID tests in the dark, captured by injecting a forward current of (a) 0.5 A and (b) 1.0 A.

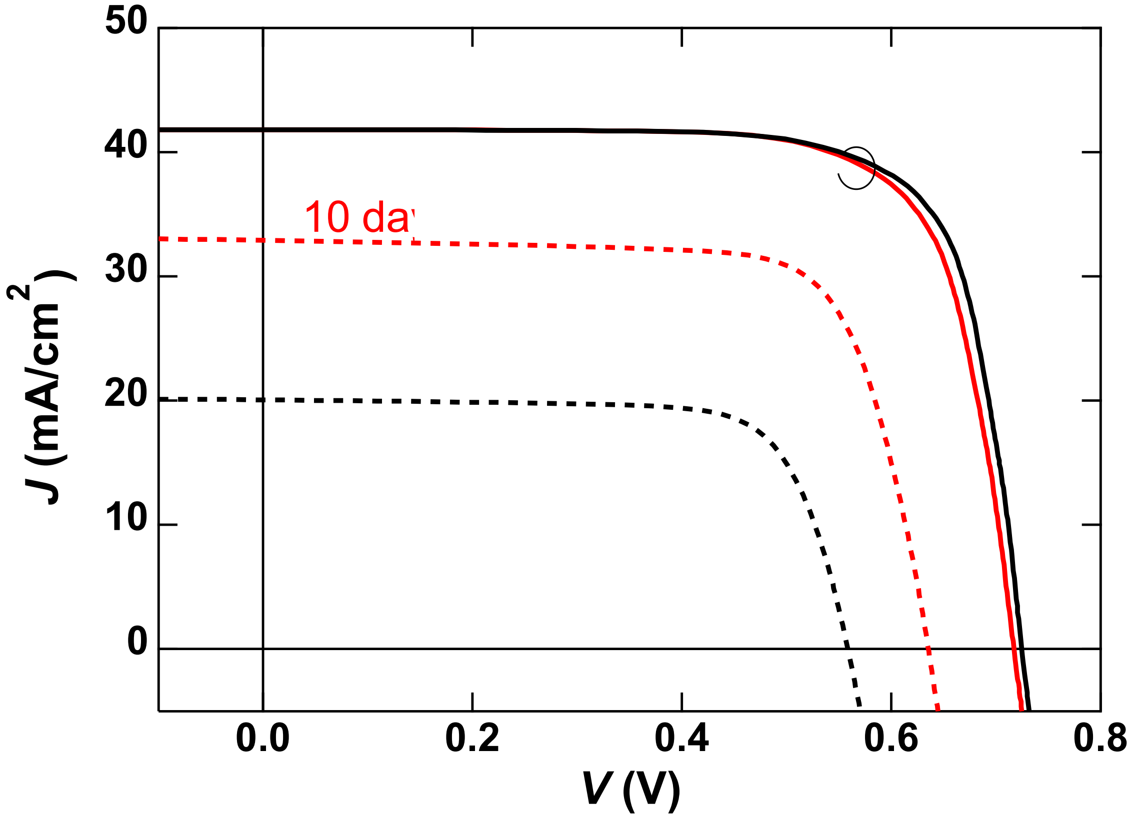

Figure 1 Y. Xu et al.,

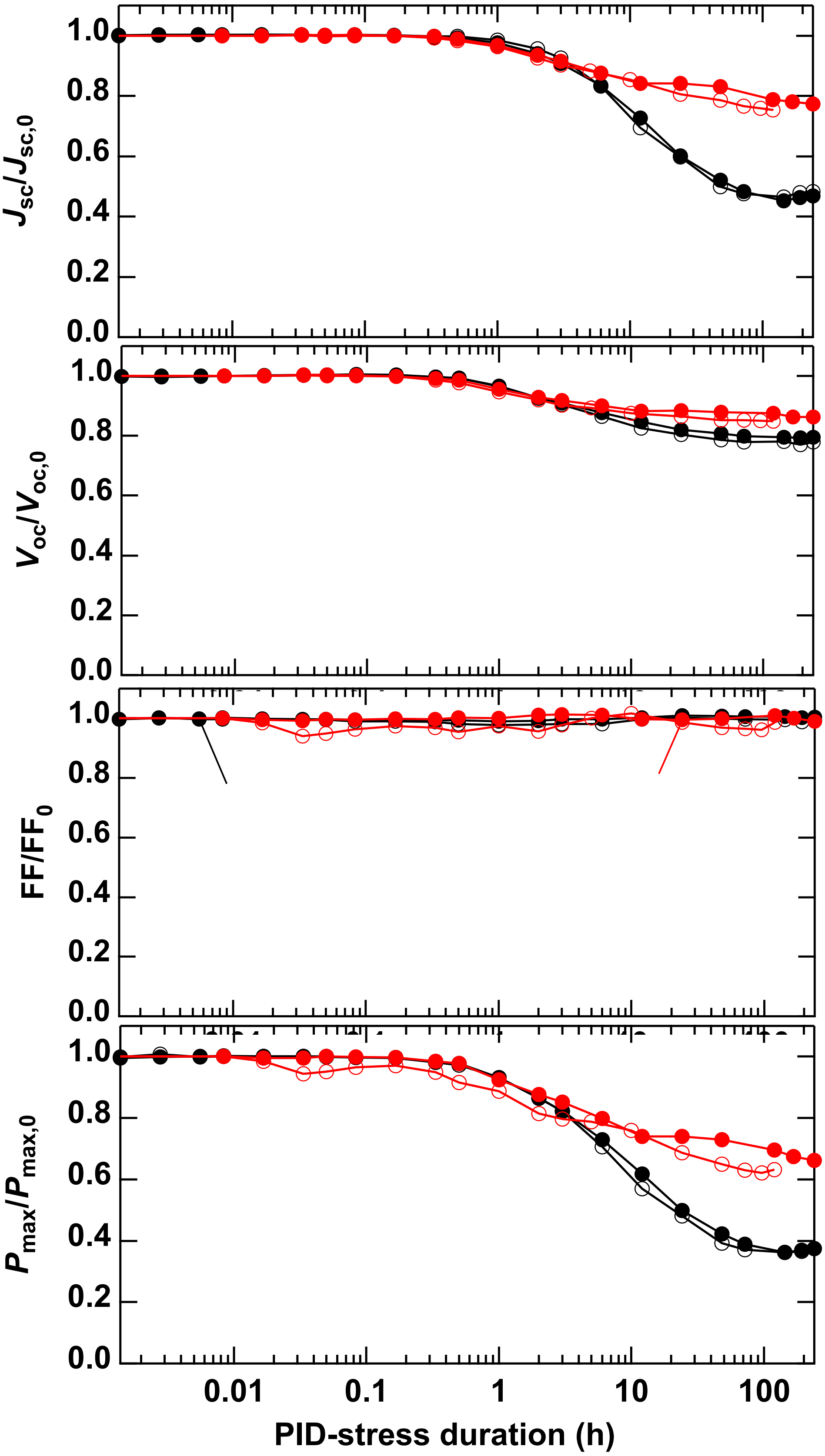

Fig. 2 Y. Xu et al.,

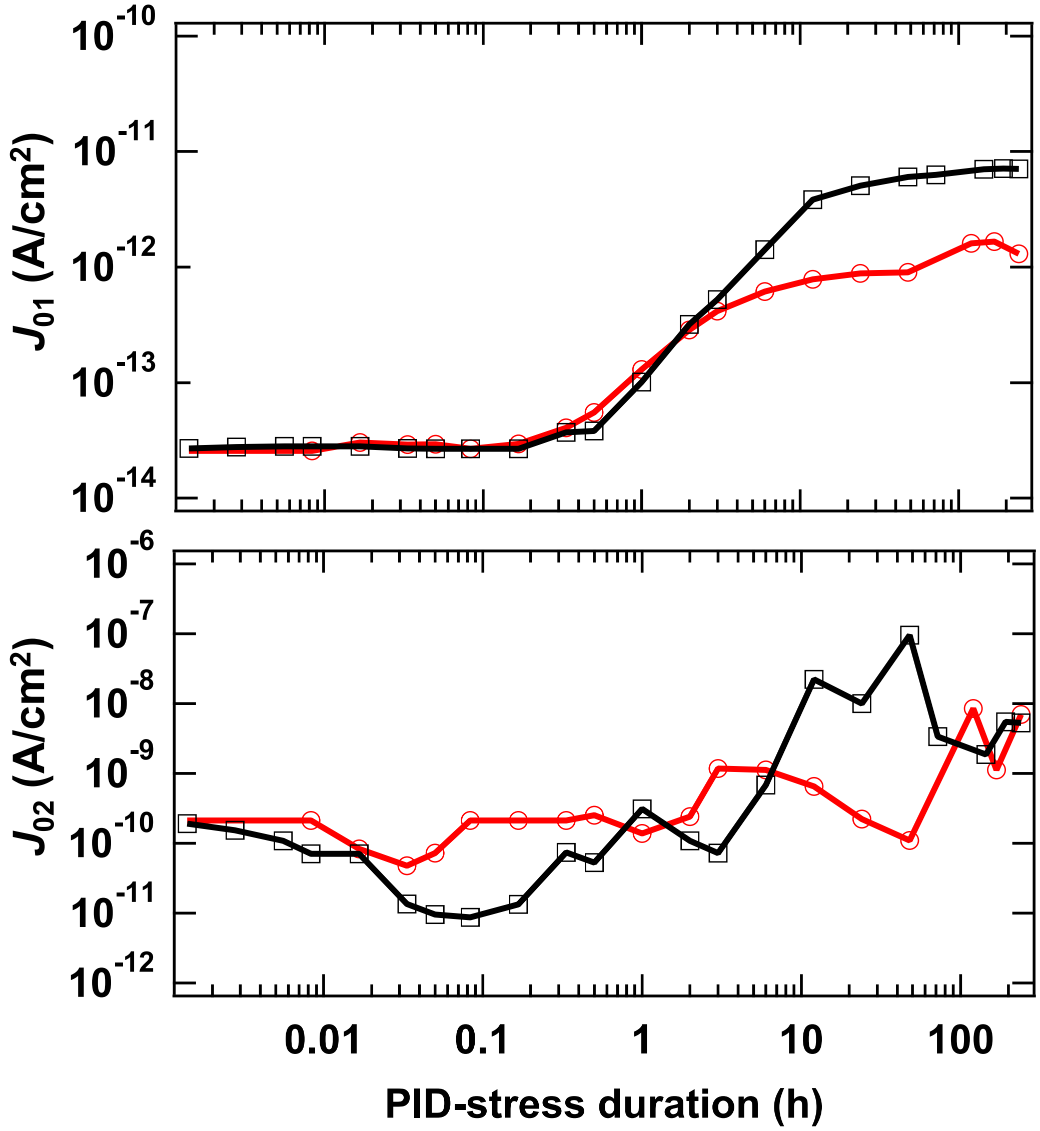

Fig. 3 Y. Xu et al.,

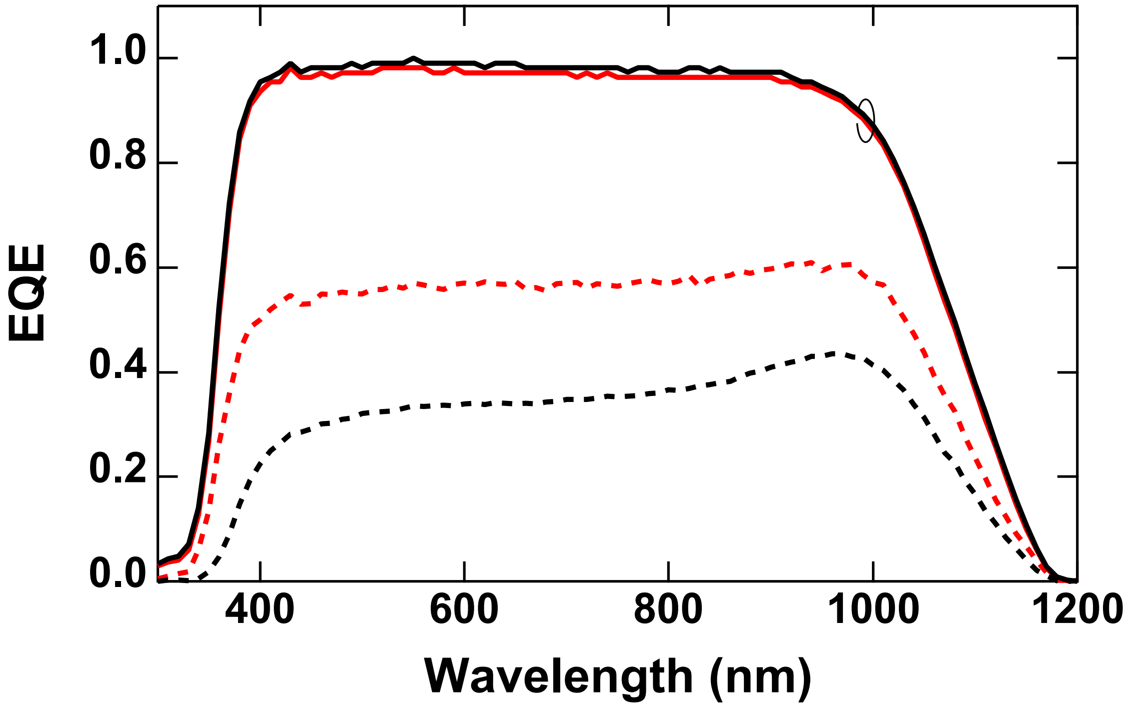

Fig. 4 Y. Xu et al.,

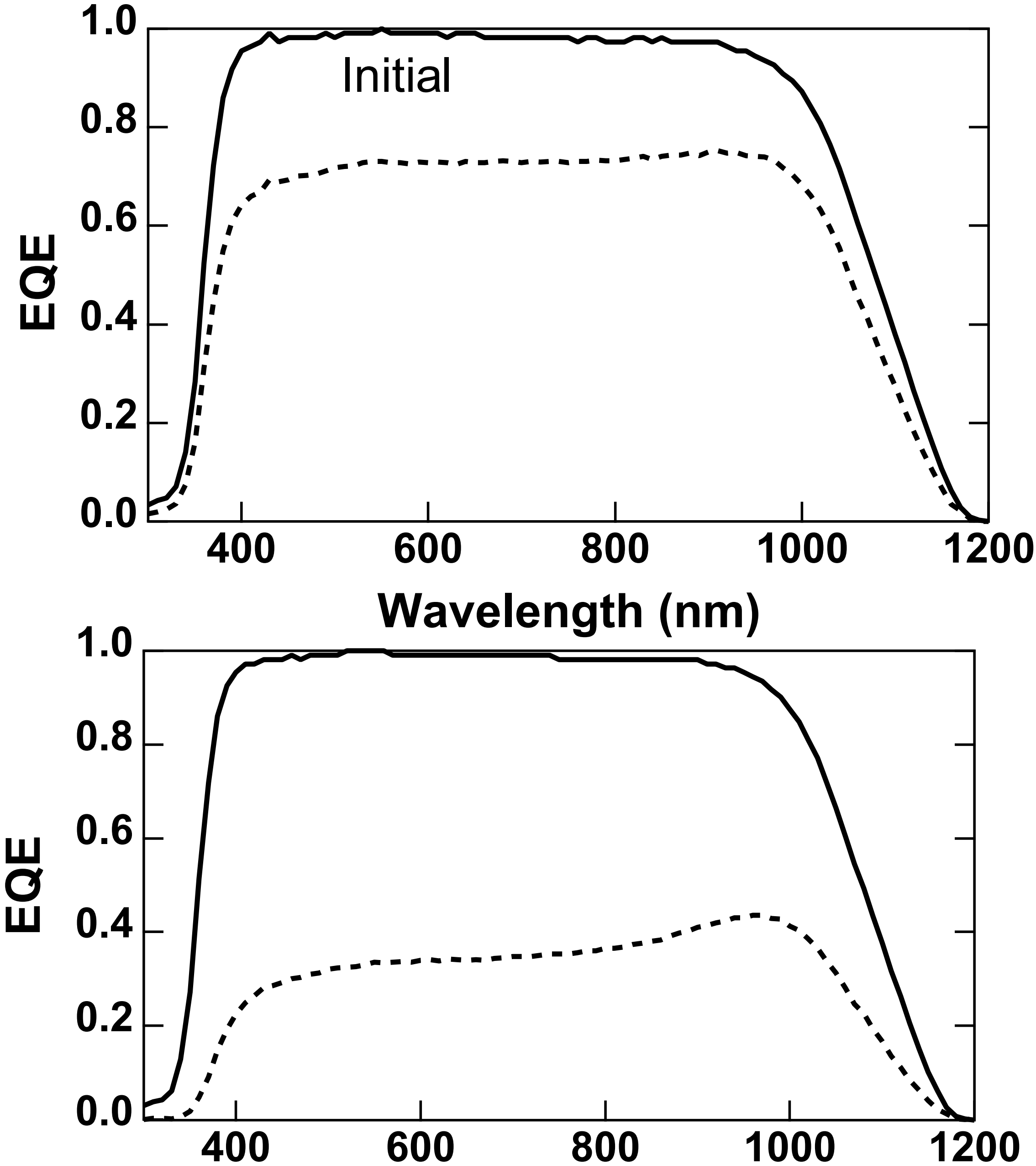

Fig. 5 Y. Xu et al.,

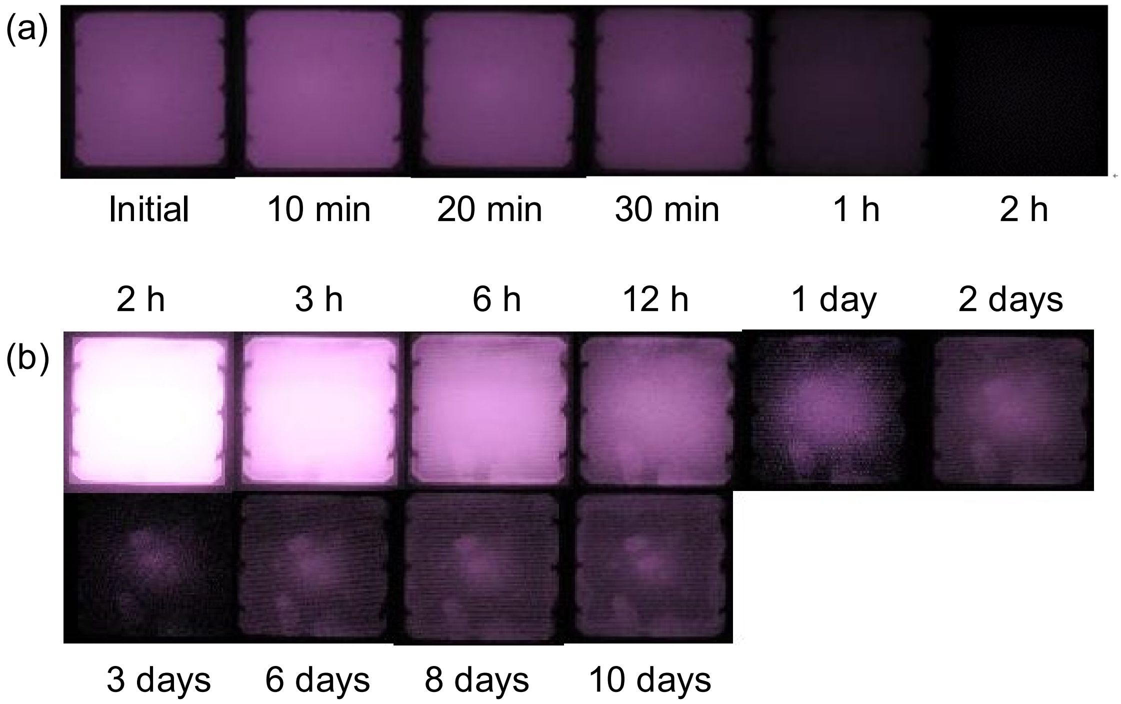

Fig. 6 Y. Xu et al.,